

Comparison Between Parameters of Corrosion, Obtained by Destructive and Non-destructive Electrochemical Techniques

Caroliny Alves¹, Andrielli M. Oliveira^{1*}, Tiago Cardoso¹ and Oswaldo Cascudo¹

¹GEDur - Durability Study Group, LABITECC - Laboratory of Technological Innovation in Civil Construction Civil and Environmental Engineering School, Federal University of Goiás - UFG),
74.605-220. Praça Universitária, Goiânia – GO, Brazil.

carolinyalves@discente.ufg.br, andriellimorais@ufg.br (corresponding author),
thiagocostacardoso@gmail.com, ocascudo@gmail.com

Abstract. *This research aims to compare corrosion parameters obtained by linear polarization technique and Tafel extrapolation method in steel bars embedded in concrete. It was analyzing the intervention of mineral additions, such as metakaolin (10%) in binary concrete mixtures and silica fume (9%) and nano silica (1%) in ternary concrete mixtures of water/binder ratio of 0.4 and 0.6 after induction of corrosion by wetting and drying cycles in a solution containing chlorides. Thus, the corrosion potential (E_{corr}), polarization resistance (R_p) and corrosion rate (i_{corr}) were measured. As a main result, a good correlation (R^2 of 0.82 and 0.96) was obtained with the values of polarization resistance (R_p) and corrosion rate (i_{corr}), obtained by R_p and by Tafel slope, respectively. Binary and ternary concretes mixtures showed higher performance than reference concretes. Reference concrete with w/ratio of 0.6 showed a high corrosion rate.*

Keywords: *Corrosion, mineral additions, Chlorides, Linear polarization technique, Tafel extrapolation method.*

1 Introduction

It has been that the corrosion can reduce the service life of concrete structures reinforcing with steel bars. In this sense, it was reported in industrialized countries that the total price of repairing corroded structures is about 4% of the gross domestic product (GDP) (François, Laurens and Deby 2018).

The use of greater cover thicknesses, lower water/binder ratios (w/b) and the incorporation of supplementary cementitious materials have been shown to be efficient in protecting the reinforcement against the entry of chlorides, especially in binary and ternary mixtures. These mineral additions can reduce the porosity and delay the entry of gases, moisture, chloride and other ionic species into to the concrete (Figueiredo et al. 2014, Oliveira and Cascudo 2018, Ghanei et al. 2020, Oliveira et al. 2020, Oliveira et al. 2022a and 2022b; Oliveira et al. 2023, Cascudo et al. 2021, Han et al. 2023).

At the same time, parameters obtained from electrochemical techniques can be used in the evaluation, control and investigation of steel corrosion, besides of providing information for scheduled maintenances or not in reinforced concrete structures. However, the correlation between corrosion parameters, mainly polarization resistance (R_p) and corrosion rate (i_{corr}), obtained through destructive (Tafel slope) and non-destructive (polarization resistance - R_p or linear polarization) techniques is still restricted.

Therefore, this paper aims focuses on comparing parameters of corrosion obtained by linear

polarization technique or polarization resistance (R_p) and by Tafel extrapolation method in steel bars embedded in concrete. It was studying the interference of supplementary cementitious materials, as the metakaolin (10%) in binary concrete mixtures and silica fume (9%) and nano silica (1%) in ternary concrete mixtures of water/binder ratio of 0.4 and 0.6 after 300 days of induction of corrosion through wetting and drying weekly cycles in a solution rich in chlorides at a concentration of 5%. For this, the corrosion potential or half-potential cell (E_{corr}), polarization of resistance (R_p) and corrosion rate (i_{corr}) were measured.

The main contribution of this research is the correlation between kinetic parameters obtained by R_p technique and Tafel slope. Also, the relevant point of contribution is to highlight the extraordinary role played by mineral additions in terms of protecting the reinforcement against electrochemical corrosion induced by chloride ions.

2 Experimental Program

2.1 Materials, Concretes and Specimen

Brazilian-type CP II F-40 Portland cement (composed of 75–89% clinker and calcium sulphate, and 11–25% in mass of limestone filler, similar to the European CEM II/A-L 42,5 R, was used throughout the investigations. Besides that, natural sand of quartz origin with a fineness modulus equal to 2.40 and specific mass 2.64 g/cm³ and coarse aggregate from the crushing of granitic rock with a fineness modulus 6.57 and specific mass 2.72 g/cm³ were used.

Concrete compositions used in this investigation were defined based on previous work (Cascudo et al. 2020). The primary variables adopted in this research were the water/binder ratio (w/b) and type of concrete. Concrete mixtures were cast with two w/b ratios: 0.4 and 0.6, following the Brazilian standard NBR 6118: 2014, regarding the maximum water/binder ratio established for reinforced and prestressed concrete structures in environments with strong environmental aggressivity and high risk of deterioration of these structures. Moreover, the fixed contents of Portland cement mass replacement by additions were silica fume (9%) and nano-silica (1%) (SN) and with 10% metakaolin (MM). Also, concrete without mineral additions were produced (REF). The criteria for choosing these levels were published by the literature (Oliveira and Cascudo 2018 and Cascudo et al. 2021). Table 1 shows the composition of concretes studied.

Table 1. Mixture proportions of the concretes studied (kg/m³).

Concrete	Water binder /ratio	Cement (kg/m ³)	Unit mix (kg)			Compressive strenght (MPa)	
			Cement	Mineral addition	Aggregates		
					Fine	Coarse	
REF4	0.4	365	1	0.00	2.37	2.76	50
REF6	0.6	260	1		3.55	3.73	35
SN6	0.6	234	1	0.01 Nano silica and 0.09 silica fume	3.53	3.71	40
MM4	0.4	330	1	0.10	2.36	2.75	66
MM6	0.6	236	1	Metakaolin	3.54	3.72	37

Cubic concrete specimens were produced with dimensions of 150 mm of side and they were

reinforced with four longitudinal rebars of 10 mm of nominal diameter and specific area delimited for corrosion. After manufacturing, the test specimens were under cure for 28 days in a controlled room (temperature of $22 \pm 2^\circ\text{C}$ and a minimum relative humidity of 95%). Thereafter, the specimens remained until the age of testing in the laboratory environment, which corresponded to the age of 91 days.

2.2 Corrosion Induction by Wet–dry cycles in NaCl Solution and Corrosion Parameters Measured by Electrochemical Techniques

From 91 days to 300 days, the corrosion procedure was induced by wet–dry cycles in NaCl solution (NaCl diluted to 5% by mass or 0.855 M). The weekly cycles were 2 days of partial immersion of the specimen until 7.5 cm (2.95 inches) of its height in NaCl aggressive solution and subsequent drying during 5 days in a controlled environment (40°C of temperature and $50 \pm 5\%$ of relative humidity). Concrete specimens were subjected to total of 30 cycles or 209 days of attack in aggressive solution containing chlorides. The specimens remained from 300 to 1920 days of the age in the laboratory environment. At the age of 1927 days, the specimens were conducted to electrochemical tests after 7 days in climatic chamber.

Thermodynamic and kinetic aspects of steel bars corrosion embedded in the concretes were evaluated by means of the techniques of corrosion potential (E_{corr}) and polarization of resistance (R_p), the latter making it possible to estimate the instantaneous corrosion rate (i_{corr})

In addition, the Tafel extrapolation method was employed. Figure 1 shows electrochemical experimental setup used. In order to avoid interferences from external electric fields, all the measuring apparatus were inserted inside a Faraday cage, where all the electrochemical measurements were taken.

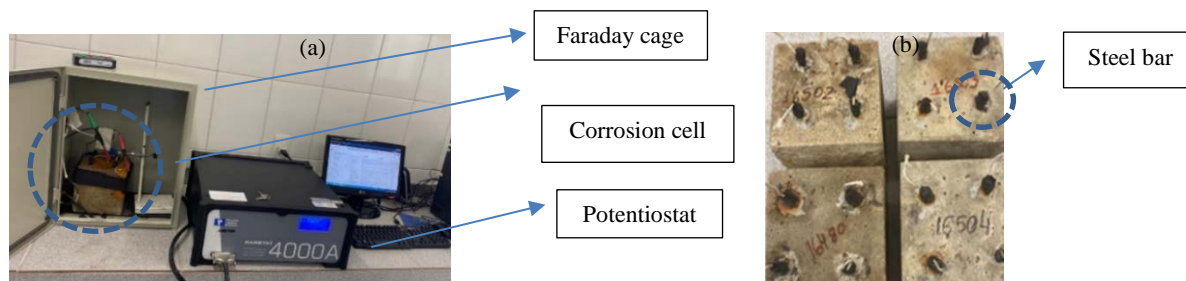


Figure 1. Experimental setup used in the corrosion measurements: (a) detail of corrosion cell connected to potentiostat and computer and (b) detail working electrode (rebars embedded in concrete) with electrical connections.

The electrochemical measurements were performed by means of a three electrode arrangement using a potentiostat model Parstat 4000A, managed by Ziew4 e VersaStudio software version 2.63.3.0. A working electrode (rebars embedded in concrete) (Fig 1b), a saturated calomel electrode – SCE (as the reference electrode) and a counter electrode of stainless steel (externally in contact with one of the faces of the concrete test specimen) were connected to the potentiostat. Each specimen had 4 rebars embedded in concrete.

The criteria of ASTM C 876-22b: 2022 were considered for corrosion potential (E_{corr} , mV). These criteria consider that if E_{corr} is more positive than -126 mV (SCE), the steel bars are

passives and the probability of corrosion is smaller than 10%. As well, if E_{corr} is more negative than - 276 mV (SCE), it considers that the corrosion on the steel bars has probability of 90% to happening. Finally, there is a range of uncertainty with E_{corr} from -126 mV to -276 mV (SCE).

The polarization resistance (R_p) was determined by applying a small potential shift of steel rebar and by recording the current induced. The parameters used were: ± 10 mV of polarization, scan rate of 10 mV/min or 0.167 mV/s (scanning in the anodic direction) and ohmic drop compensation of dynamic type (ASTM G59-97:2020). From the R_p value, the corrosion current density (i_{corr}) could be calculated by Stern–Geary equation (Equation 1). According to Faraday’s Law (Poupard et al. 2004), corrosion current density (in $\mu\text{A}/\text{cm}^2$, for example) can be related to corrosion rate data, such as: millimeters per square decimeter per day (mdd) or millimeters per year (mmpy). Because of this, corrosion current density data are usually employed as corrosion rate data, as used in the present work.

$$I_{\text{corr}} = \frac{B}{R_p} \quad (1)$$

The proportionality factor (B - Stern-Geary constant) used varies from 13 to 52 mV. For measurements in reinforced concrete specimens, as established by Andrade and Alonso 1991, it was adopted a value of 26 mV for corroding steel and a value of 52 mV for passive steel.

It should be noted that to obtain the corrosion current intensity densities (I_{corr}) in μA , using the R_p technique, the Stern-Geary equation was used, described in Equation 1.

For obtaining the value of "B", by the Tafel slope, it was based on Equation 2, with polarization with ± 250 mV e I_{corr} was calculated by software.

$$B = \frac{\beta_a * \beta_c}{2,3 * (\beta_a + \beta_c)} \quad (2)$$

Where β_a and β_c refer to the anodic and cathodic Tafel constants, respectively. To obtain i_{corr} values, in $\mu\text{A}/\text{cm}^2$, Equation 3 was used. The parameter “A” refers to the surface area exposed to corrosion by the working electrode equal value to 12.88 cm^2 .

$$i_{\text{corr}} = \frac{I_{\text{corr}}}{A} \quad (3)$$

For the evaluation of the corrosion rate (i_{corr}) of the steel reinforcements, the criteria of Andrade and Alonso (2001) were adopted.

Table 2. Corrosion rate (i_{corr}): criteria of Andrade and Alonso (2001) adopted.

Corrosion level	Corrosion rate	
	$\mu\text{A}/\text{cm}^2$	$\mu\text{A}/\text{year}$
Negligible	<0.1	<1.15
Start of active corrosion	$\cong 0.2$	$\cong 2.2$
Low	0.1 a 0.5	1.1 a 5.75
Moderate	0.5 a 1.0	5.75 a 11.5
High	>1.0	> 11.5

3 Results and Discussion

3.1 Thermodynamic and Kinetic Parameters of Corrosion

Table 3 shows the average results of 4 steel bars for each type of concrete.

All concretes showed E_{corr} with a corrosion probability greater than 90%, according to ASTM C876-22b: 2022. The corrosion rates were obtained directly from the Versa Studio software by R_p and Tafel slope techniques. The MM4 and REF4 concretes showed better performance due to low values of corrosion rates, follow for SN6 and MM6 concretes by R_p technique. This designates a cementitious system with good capacity to protect the reinforcement, since the value of R_p denotes the inertia that the system has in developing the electrochemical corrosion process.

On the other hand, i_{corr} by Tafel extrapolation method showed some differences, calculated by software, in SN6 and MM6 concretes.

Table 3. Thermodynamic and kinetic Corrosion Parameters obtained from resistance polarization (R_p) technique and Tafel extrapolation method.

Concrete	R_p technique			Corrosion degree R_p technique	Tafel curves technique.				
	E_{corr} (mV)	R_p (kOhm.cm ²)	i_{corr} (μ A/cm ²)		i_{corr} (μ A/cm ²)	β_a (mV)	β_c (mV)	B (mV)	R_p (kOhms.cm ²)
REF4	-358	575.5	0.004	Negligible	0.012	1.53×10^7	34.04	14.8	163.5
REF6	-595	1.2	1.691	High	1.838	35.16	19.75	5.5	1.1
SN6	-580	47.6	0.043	Negligible	0.845	408.93	27.85	11.3	2.4
MM4	-307	420.3	0.005	Negligible	0.024	6.62×10^2	11.39	5.0	85.9
MM6	-657	42.7	0.047	Negligible	0.209	29.03	164.34	10.7	9.6

In both techniques, the highest corrosion rates, i_{corr} and lowest R_p values are observed in the reference sample with the highest water/binder content (REF6). In addition, reference concretes that show a decrease in R_p values and an increase in corrosion rates, denote a reduction in the service life and durability of the structure (OLIVEIRA; CASCUDO, 2018).

With regard to the Tafel constants, for the samples with the best performance (REF4, MM4) higher β_a values are observed. Thus, for these samples, there was a direct correlation between high values of β_a and R_p . While the magnitude of the anode constant decreases for SN6 and MM6, respectively. By symmetry, in these lower performance samples, the lowest R_p values are presented, obtained by means of Tafel Curves.

Additionally, the corrosion current density parameters (i_{corr}) were evaluated using the guidelines by Andrade and Alonso (2001), summarized in Table 2 and the correlation of results in Figure 2.

Regarding the calculation of R_p and i_{corr} , the correlation between concretes studied was drawn.

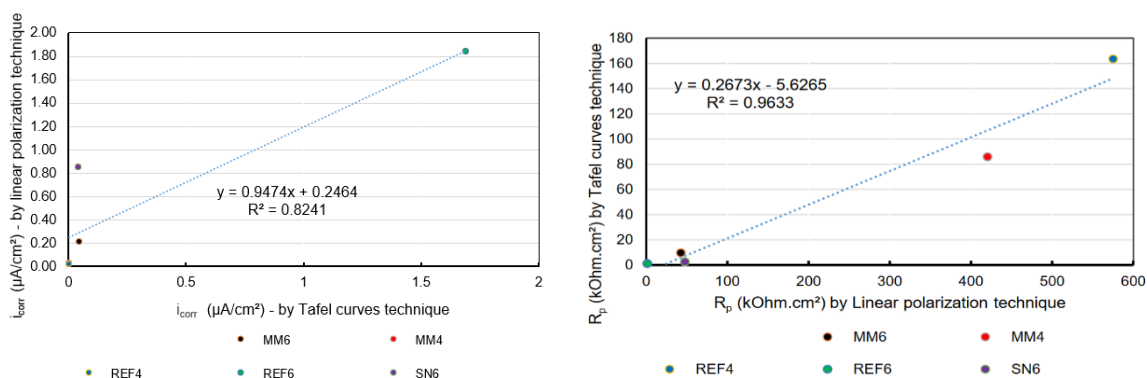


Figure 2. Values Correlation obtained by linear polarization resistance (R_p) and Tafel Curves techniques: (a) i_{corr} ($\mu\text{A}/\text{cm}^2$) (left) and (b) R_p value (right).

A relevant point regarding the comparison between the i_{corr} and R_p values results for the concrete studied was established. Good correlations with values of 0.82 and 0.95 for respective i_{corr} and R_p values between the destructive and non-destructive techniques were obtained.

It is important to point out that for the evaluation of the state of corrosion in the reinforcement (Table 2) the highest i_{corr} values of each representative sample were used. In this way, the concretes in the lowest water/binder ratio of 0.40; with and without incorporation of Metakaolin, showed negligible degrees of corrosion. On the other hand, the other system of reference with a higher water/binder ratio of 0.60 showed a high state of corrosion. However, with the addition of silica fume and nanosilica (SN6), a moderate corrosion state was presented. This result is in line with Oliveira and Cascudo (2018), since lower i_{corr} values are reported for concretes with the incorporation of mineral additions.

Thus, for more electronegative values of E_{corr} , there are greater magnitudes of i_{corr} , therefore, they are in an active corrosion state, in agreement with the results of Tang (2019). By symmetry, this behavior is reflected in the Tafel curves so that the samples that present the best performance and consequently the lowest i_{corr} magnitudes are the MM4 and REF4 samples.

This performance can be observed when analyzing the slopes and values of β_a (anodic betas) which are superior when compared to other cementitious systems. While the SN6 sample remained in a moderate state of corrosion. And the samples MM6 and REF6 showed the worst performance with high values of i_{corr} and more electronegative potential values (E_{corr}) than the other specimens of concrete.

It is observed that there is a good correlation between the calculated values of R_p , through adopted values of “B” and values obtained experimentally by Tafel curves, given that the correlation coefficient R^2 equal to 0.96 is presented. This means, roughly speaking, that it is possible to obtain the bias resistance by either method. However, using the Tafel curves, the results are more accurate.

It has been very interesting to note the extraordinary role played by mineral additions in terms of protecting the reinforcement against electrochemical corrosion induced by chloride ions even for concretes with minor compressive strength. Concretes with near compressive strength (class) had different performances, especially those containing some type of mineral addition in binary or ternary mixtures. This behavior expresses a delay the entry of gases,

moisture, chloride and other ionic species into to the concrete and more service life and performance over time.

4 Conclusions

According to this study, it is possible to conclude:

- Concretes with supplementary cementitious materials, as the metakaolin (10%) in binary concrete mixtures and silica fume (9%) and nano silica (1%) in ternary concrete mixtures showed a good behavior in delay the corrosion;
- For concretes without mineral addition, the water/binder ratio of 0.4 and 0.6 was very relevant for durability and corrosion;
- All concretes shower higher probability of corrosion (E_{corr}) with several corrosion rates (i_{corr});
- To obtain the R_p values, the “B” values described in the literature can be adopted or obtained through Tafel curves, as both present good correlation ($R^2=0.96$), according to the comparative analysis of obtaining the polarization resistance.
- There was a good correlated of i_{corr} obtained by R_p technique and Tafel curves technique ($R^2=0.82$).

Acknowledgements

This work is part of the P&D project - PD. 0394-1704-2017, regulated by the National Agency of Electric Energy - ANEEL, developed by Eletrobrás FURNAS and FUNAPE/UFG/EECA/LABITECC. The authors express their gratitude to all these partners, as well as to CNPq - Conselho Nacional de Desenvolvimento Científico e Tecnológico, CAPES - Coordenação de Aperfeiçoamento de Pessoal de Nível Superior.

ORCID

Caroliny Alves: <http://orcid.org/0000-0002-0492-445X>

Andrielli M. Oliveira: <http://orcid.org/0000-0001-8977-785X>

Oswaldo Cascudo: <http://orcid.org/0000-0003-1879-6396>

References

- American Society for Testing and Materials. ASTM C876-22b: *Standard test for half-cell potentials of uncoated reinforcing steel in concrete*. ASTM International. 2022.
- American Society for Testing and Materials, ASTM G 59 – 97: *Standard Test Method for Conducting Potentiodynamic Polarization Resistance Measurements*, Annual Books of ASTM Standards, Philadelphia, 2020.
- Andrade, C.; Alonso, C. *On-site measurements of corrosion rate of reinforcements*. Construction and Building Materials, v. 15, p. 141- 145, 2001.
- Cascudo, O. *Influência das adições minerais na durabilidade do concreto sujeito à carbonatação*. 2000. 310 f. *Tese (Doutorado em Construção Civil) – Escola Politécnica, Universidade de São Paulo, São Paulo, 2000*.
- Cascudo, O. Teodoro, R.; Oliveira, A. M.; Carasek, H. *Effect of different metakaolins on chloride-related durability of concrete*. ACI Materials Journal. v. 118, p. 3-14, 2021.
- Cascudo, O.; Pires, P.; Carasek, H.; Castro, A.; Lopes, A. *Evaluation of the pore solution of concretes with mineral additions subjected to 14 years of natural carbonation*. Cement and Concrete Composites, v. 115, p. 1/103858-13, 2020. <https://doi.org/10.1016/j.cem-concomp.2020.103858>.
- Figueiredo; C. P.; Santos, F. B.; Cascudo, O.; Carasek, H.; Cachim, P.; Velosa, A. *O papel do metacaulim na proteção dos concretos contra uma ação deletéria de investigações*. Revista IBRACON de Estruturas e Materiais, v. 7, n. 4, p. 685-708, 2014.
- François, R.; Laurens, S.; Deby, F. *Chapter 1 -Steel corrosion in reinforced concrete*. In: FRANÇOIS, R.;

- LAURENS, S.; DEBY, F. Corrosion and its consequences for reinforced concrete structures, 2018, p. 1-41.
- Ghanei, A.; Eskandari-Naddaf, H.; Ozbakkaloglu, T.; Davoodi, A. *Eletrochemical and statistical analyses of the combined effect of air-entraining admixture and micro-silica on corrosion of reinforced concrete*. Construction and Building Materials, v. 262, 2020.
- Han, X.; Wang, P.; Cui, D.; Tawfik, T. A.; Chen, Z.; Tian, L.; Gao, Y. *Rebar corrosion detection in concrete based on capacitance principle*. Measurement. v. 209, 2023.
- Oliveira, A. M.; Alves, C. ; Cascudo, O. ; Cardoso, T. C. *Influência do Tipo de Adição Mineral em Misturas Binárias e Ternárias no Ecorr, Rp, Icorr e EIS de Concretos Expostos à Condição Agressiva Contendo Cloretos*. Revista De Engenharia Da Universidade Católica De Petrópolis, v. 16, p. 46-57, 2022a.
- Oliveira, A. M.; Cascudo, O. *Effect of mineral additions incorporated in concrete on thermodynamic and kinetic parameters of chloride-induced reinforcement corrosion*. Construction and Building Materials, v. 192, p. 467-477, 2018.
- Oliveira, A. M.; Cascudo, O.; Castro, A. *Effect of the type of concrete with mineral additions on the reinforcement corrosion induced by chlorides – analyses in the same mechanical strength class*. In: XV INTERNACIONAL CONFERENCE ON DURABILITY OF BUILDING MATERIALS AND COMPONENTS – DMBC, Barcelona, Spain, 2020. Disponível em: <https://www.scipedia.com/wd/images/4/41/Draft_Content_615884159p876.pdf>. Acesso em: 03 de jul. 2022.
- Oliveira, A. M.; Silva, C. A. ; Cascudo, O. *Uso de Técnicas Eletroquímicas para Avaliação da Corrosão de Armaduras no Concreto: uma Revisão Sistemática da Literatura de 1993 A 2021*. In: Congresso Internacional de Construção Civil, 2022, On-line. Congresso Internacional de Construção Civil, Brasília, Distrito Federal, 2022b. v. 1.
- Oliveira, A. M ; Oliveira, A.P. Domingos, J.V.; Neves Júnior, A. ; Cascudo, O. *Study of the development of hydration of ternary cement pastes using X-ray computed microtomography, XRD-Rietveld method, TG/DTG, DSC, calorimetry and FTIR techniques*, Journal of Building Engineering, Volume 64, 2023,105616, ISSN 2352-7102, <https://doi.org/10.1016/j.jobee.2022.105616>.
- Tang, k. *Stray alternating current (AC) induced corrosion of steel fibre reinforced concrete*. Corrosion Science, v. 152, p. 153- 171, 2019.